Molecular Beacons

DOI: 10.1002/anie.200803549

Low-Noise Stemless PNA Beacons for Sensitive DNA and RNA Detection**

*Elke Socher, Lucas Bethge, Andrea Knoll, Nadine Jungnick, Andreas Herrmann, and Oliver Seitz**

Fluorescent probes that signal the presence of specific nucleic acids are required in a variety of bioassays, including DNA quantification, SNP typing (SNP = single-nucleotide polymorphism), and analysis of mRNA expression in living cells.[1] The majority of probes take advantage of the distance-dependent interaction between two chromophores. Sensitive fluorescent hybridization probes show large hybridization-induced enhancements of fluorescence emission, which may reach signal-to-background ratios (SBR) on the order of 10^2.[2] Selective probes enable single-nucleotide-specific fluorescence signaling. Success in both sensitive and specific DNA and RNA detection has been achieved using DNA molecular beacons (MBs, Scheme 1 A).[3] These hairpin-shaped probes have been designed to bring the two interacting dyes into close proximity. The SBR is high, because in the absence of target the fluorescence is efficiently quenched by fluorescence resonance energy transfer (FRET), collisional quenching, and/or formation of ground- or excited-state complexes. Molecular beacons bind target DNA with high match/mismatch specificity, but only within a certain temperature range that depends on the difference between thermal stabilities of matched and mismatched probe–target complexes.[4] It is, thus, impossible to distinguish matched from mismatched targets at conditions for which both matched and mismatched probe–target complexes co-exist.

The major limitation in molecular-beacon design is that features that increase sensitivity are detrimental to the sequence specificity of fluorescence signaling and vice versa. Large fluorescence enhancements can only be obtained when the stem region is readily opened, while high specificity calls for stable stems that resist opening by mismatched hybridization. We envisioned an alternative beacon design. The approach on one hand retains a signaling mechanism used in molecular beacons, wherein two chromophores detect changes of probe conformation, but it omits the requirement for the formation of stable hairpin structures.[5] On the other hand, "smart" labels are used that become fluorescent and initiate FRET to a near-infrared dye only when the donor dye is embedded in perfectly matched base pairs. It is shown that the combination of the two processes, detection of conformational changes by a switch in energy transfer mechanisms and signaling of altered stacking interactions of an intercalator dye, allows for up to 108-fold fluorescence intensification upon hybridization. Importantly, the stemless probes distinguish matched from mismatched targets at virtually any temperature. Homogeneous detection of both DNA and RNA targets is demonstrated.

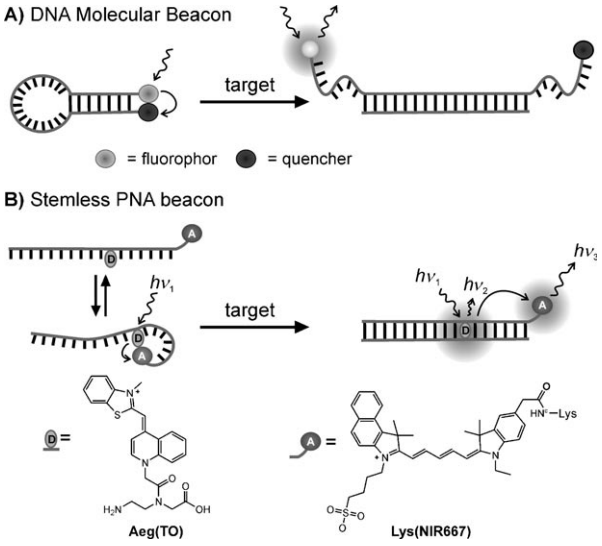

Scheme 1. Comparison of A) molecular beacons with B) stemless FIT–PNA beacons in the detection of complementary nucleic acids. In stemless FIT–PNA beacons, an intercalator dye such as thiazole orange (TO) serves as a base surrogate that signals stacking against matched base pairs by FRET to a near infrared dye such as NIR667.

The design approach is illustrated in Scheme 1 B. An intercalator dye, such as thiazole orange, is introduced as base surrogate in a peptide nucleic acid (PNA)-based probe and used as donor for FRET. A terminally appended near-infrared (NIR) dye, such as NIR667, serves as acceptor dye. It was expected that excitation of the donor in single-stranded probes would induce negligible emission of the acceptor dye because 1) the donor excited state is rapidly depleted owing to torsional motion around the central methine bridge of unstacked thiazole orange,[6] 2) the NIR667 (acceptor) dye is quenched upon collisions with nucleobases, and 3) intramolecular dye–dye dimers or short-lived collision complexes may form, aided by the tendency of the uncharged, hydrophobic PNA molecule to adopt a collapsed structure in

[*] E. Socher, L. Bethge, Dr. A. Knoll, Prof. Dr. O. Seitz
Institut für Chemie der Humboldt-Universität zu Berlin
Brook-Taylor-Strasse 2, 12489 Berlin (Germany)
Fax: (+49) 30-2093-7266
E-mail: oliver.seitz@chemie.hu-berlin.de
N. Jungnick, Prof. Dr. A. Herrmann
Institut für Biologie der Humboldt-Universität zu Berlin
Invalidenstrasse 42, 10115 Berlin (Germany)

[**] We acknowledge support from the Deutsche Forschungsgemeinschaft and Schering AG.

Supporting information for this article is available on the WWW under http://dx.doi.org/10.1002/anie.200803549.

© 2008 Wiley-VCH Verlag GmbH & Co. KGaA, Weinheim

water.[5c,d] In the double strand, excitation of the donor was envisioned to prompt acceptor emission, because 4) the donor is turned on owing to the restriction of torsional motion upon stacking of thiazole orange against the formed base pairs,[5b,f,7] 5) the distance between the donor and the acceptor is sufficiently low to permit FRET (less than 30 Å), and 6) the rigidity of the formed double helix hampers quenching caused by donor–acceptor or acceptor–nucleobase contacts. Furthermore, the known responsiveness of the TO dye to distortions of local duplex structure should also prevail in energy-transfer processes. In a mismatch environment, the TO "base" fluoresces poorly because it has room for twisting motions.[6] It should thus be feasible to discriminate mismatched targets beyond the thermal stability of probe–target complexes.

The probe system shares one feature with recently disclosed FIT probes (FIT = forced intercalation): the use of an intercalating cyanine dye as artificial nucleobase.[5f] Yet, we expected that the interaction of the intercalator with a second carefully chosen dye would substantially increase the sensitivity. We first explored model sequences **1**, **2**, and **3** (Figure 1) as examples for donor-only labeled probes (**1D**, **2D**, **3D**) that showed different abilities in producing fluorescence enhancement upon hybridization. The analysis of fluorescence spectra measured before and after hybridization with matched DNA revealed that the attachment of the NIR acceptor dye in donor–acceptor-labeled probes **1DA**, **2DA**, and **3DA** increased the sensitivity by one order of magnitude. For example, the TO dye in probe **1D** has been shown to confer a high sensitivity, characterized by a strong fluorescence enhancement $F_{ss}/F_{ds} = 24$, upon matched hybridization with DNA ODN**1** (Figure 2A).[6a] The donor–acceptor-labeled probe **1DA** proved even more sensitive owing to a very low fluorescence background. The single-strand emission quantum yield of TO in **1DA** was decreased by 98% from $\phi_{ss} = 0.0239$ to $\phi_{ss} = 0.0004$ (Table 1). The simultaneous decrease of quantum yield of NIR667 emission in **1DA** ($\phi_{ss} = 0.005$ as opposed to $\phi_{ss} = 0.03$ of acceptor-only probe **1A**) suggests a contact-based mechanism of fluorescence quenching. Further support was provided by UV/Vis spectra, which revealed a red shift of the major absorption peaks of both TO and NIR667 (see Figure S15 in the Supporting Information). Such changes in the shape of the absorption spectrum indicate that ground-state interactions contribute to the quenching of TO and NIR667 emission.[8] The melt analysis showed only insignificant changes of the melting

PNA:

1, **X**-gccgta-**Y**-atagccg-Gly^{CONH_2}

2, **X**-gccgtc-**Y**-ttagccg-Gly^{CONH_2}

3, **X**-gccgta-**Y**-ctagccg-Gly^{CONH_2}

1-3D, **X** = Ac, **Y** = Aeg(TO);
1-3DA, **X** = Lys(NIR), **Y** = Aeg(TO);
1-3A, **X** = Lys (NIR), **Y** = a

DNA:

ODN**1M**, 5'-CGGCTATT**M**ACGGC-3'

ODN**2**, 5'-CGGCTAATGACGGC-3'

ODN**3**, 5'-CGGCTAGTTACGGC-3'

ODN**1**, **M** = T, ODN**1G**, **M** = G;
ODN**1A**, **M** = A; ODN**1C**, **M** = C

MB:

MB**1**, 5'-Cy5-*GCACAGGC*CGATGCCGATAAATGCCGAT*GCCTGT-GC*-FAM-3'

ODN**4M**, 5'-ATCGGCATT**M**ATCGGCATCG-3'

ODN**4**, **M** = T, ODN**4G**, **M** = G; ODN**4A**, **M** = A; ODN**4C**, **M** = C

Figure 1. Test sequences used in this study.

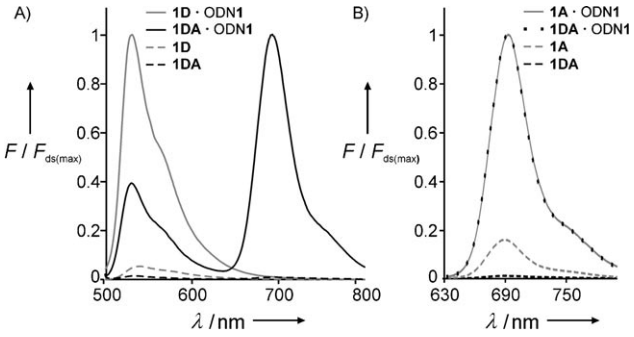

Figure 2. Normalized fluorescence spectra of **1D**, **1DA**, and **1A** before and after addition of matched ODN**1** upon excitation of A) TO ($\lambda_{Ex} = 485$ nm) and B) NIR667 ($\lambda_{Ex} = 620$ nm). Conditions: 1 μM probe and target in 100 mM NaCl, 10 mM NaH_2PO_4, pH 7.0 at 25 °C. *F* ($F_{ds(max)}$), fluorescence intensity (at emission maximum of double strand).

Table 1: Fluorescence quantum yield and fluorescence enhancement of donor-labeled probes **D**, donor–aceeptor-labeled probes **DA**, and acceptor-labeled probes **A**.[a]

PNA: **X**-gccgt**k**-**Y**-**l**tagccg-Gly^{CONH_2}
DNA: $^{3'}$CGGCA**M**-T-**N**ATCGGC$^{5'}$

		D		**DA**						**A**	
		Y = Aeg(TO); **X** = Ac		**Y** = Aeg(TO); **X** = Lys(NIR667)						**Y** = a; **X** = Lys(NIR667)	
		$\lambda_{ex} = 485$ nm		$\lambda_{ex} = 485$ nm		$\lambda_{ex} = 620$ nm		$\lambda_{ex} = 485$ nm		$\lambda_{ex} = 620$ nm	
Seq.	k-M, l-N	Φ_α	$F^{[b]}_{ds}/F^{[b]}_{ss}$	$\Phi_{\alpha(Q)}$	$F^{[b]}_{ds}/F^{[b]}_{ss}$	$\Phi_{Q(\alpha)}$	$F^{[c]}_{ds}/F^{[c]}_{ss}$	$\Phi_{Q(FRET)}$	$F^{[c]}_{ds}/F^{[c]}_{ss}$	Φ_Q	$F^{[c]}_{ds}/F^{[c]}_{ss}$
1	a-T, a-T	ss: 0.0239 ds: 0.3057	24	ss: 0.0004 ds: 0.0126	28	ss: 0.0050 ds: 0.1138	89	ss: 0.0012 ds: 0.0539	108	ss: 0.0307 ds: 0.2399	4.6
2	c-G, t-A	ss: 0.2004 ds: 0.3011	1.2	ss: 0.0043 ds: 0.0123	7	ss: 0.0126 ds: 0.1318	15	ss: 0.0026 ds: 0.0864	13	ss: 0.0473 ds: 0.2115	3.4
3	a-T, c-G	ss: 0.0255 ds: 0.2524	5	ss: 0.0009 ds: 0.0133	12	ss: 0.0064 ds: 0.0184	36	ss: 0.0022 ds: 0.0875	39	ss: 0.0112 ds: 0.0789	1.9

[a] For measurement conditions, see Figure 2. [b] $\lambda_{em} = 530$ nm. [c] $\lambda_{em} = 691$ nm. The error in the determination of the the quantum yield was estimated as 10%.

 © 2008 Wiley-VCH Verlag GmbH & Co. KGaA, Weinheim

temperature (T_m (**1DA**·OND**1**) = 75 °C, T_m (**1D**·OND**1**) = 73 °C), which suggests that the dye–dye association is too weak to affect the binding affinity of the PNA probe. In the hybridized form, both TO and NIR667 became fluorescent, as characterized by the 32- and 23-fold increases of the quantum yields ϕ_{ds} of TO and NIR667 emission, respectively, which supported the notion that contact-based quenching was no longer able to operate in the formed double helix. As a consequence of FRET, formation of the probe–target duplex was accompanied by a shift of the maximum of fluorescence from 530 to 693 nm. Most remarkable was that hybridization of **1DA** resulted in 108-fold intensification of NIR667 emission when excited at the TO absorption wavelength.

The probes **2DA** and **3DA** provided further examples wherein the introduction of NIR667 as acceptor for energy transfer from TO improved the sensitivity by one order of magnitude. For example, the presence of the NIR667 dye in **2DA** again reduced fluorescence noise in the single-stranded form of **2D** by 98% (Table 1, see also Figure S12 in the Supporting Information). Likewise, the TO/NIR667-labeled probe **3DA** provided a 39-fold increase of the FRET signal upon hybridization, whereas donor-only probe **3D** allowed only modest fivefold fluorescence intensification ($F/F_0 = 5$) upon hybridization (see Figure S13 in the Supporting Information).

One aim of this study was to develop probes that combine high sensitivity in nucleic acid detection with high specificity even under nonstringent conditions. Probe **1DA** was hybridized with matched and single mismatched targets ODN**1** and ODN**1G**, respectively. Readout of TO emission or FRET-induced NIR667 emission at 25 °C revealed that the addition of matched DNA resulted in a sevenfold stronger signal than addition of mismatched ODN**1G** (Figure 3A). Other mismatches (in ODN**1A** and ODN**1C**) were also discriminated, even though both matched and single mismatched probe–target complexes coexist at this low temperature. Probe **2DA** allowed even better mismatch discrimination at nonstringent conditions, while **3DA** showed lower (twofold) selectivity (Table S1 in the Supporting Information). The highest specificity is obtained when both the selectivity of the TO dye and the selectivity of probe–target recognition were combined. At 65 °C and in the presence of matched target ODN**1**, probe **1DA** furnished a 25-fold higher TO signal than in the presence of mismatched target ODN**1G** (Figure 3C). The NIR667 fluorescence of single mismatched duplexes was almost as high as that of perfectly matched duplex **1DA**·ODN**1** (Figure 3A). Thus, direct excitation of the terminally appended NIR667 dye provided an emission signal that responds to hybridization but not to perturbations of duplex structure such as those imposed upon mismatched base pairing.

It is instructive to compare the specificity of fluorescence signaling provided by stemless PNA beacons such as **1DA** with the specificity of DNA molecular beacons (Scheme 1) that bind the same target sequence. The FAM and Cy5 fluorophors were selected because their emission appears at similar spectral ranges as TO and NIR667 emission, respectively. We screened three MB structures for highest match/mismatch selectivity at 65 °C (see Figure S18 in the Supporting Information). This procedure required an extension of the probe sequence and a relatively long (8 bp) stem region (underlined) in MB**1** (Figure 1). As expected, MB**1** exhibited low FAM emission, which intensified as matched target ODN**4** was added (Figure S21). The hybridization experiments with single mismatched targets ODN**4G**, ODN**4A**, and ODN**4C** revealed an insufficient discrimination of mismatched target at conditions under which both matched and single mismatched probe–target duplexes are formed (Figure 3B). This behavior was expected, as the specificity of fluorescence signaling by MBs draws upon the selectivity of probe–target recognition. In contrast, stemless PNA beacons such as **1DA** allow single-nucleotide-specific fluorescence signaling even at nonstringent conditions (Figure 3A) owing to the environmental sensitivity of the TO fluorescent base surrogate. The specificity of MB**1** is uncovered at elevated temperatures (60–70 °C) near the T_m of the formed probe–target duplexes (Figure 3D). The examined specificity factor $(F_{ma}-F_0)/(F_{mi}-F_0)$ is independent of the dynamic signaling range and should, thus, not be affected by the choice of fluorophores.

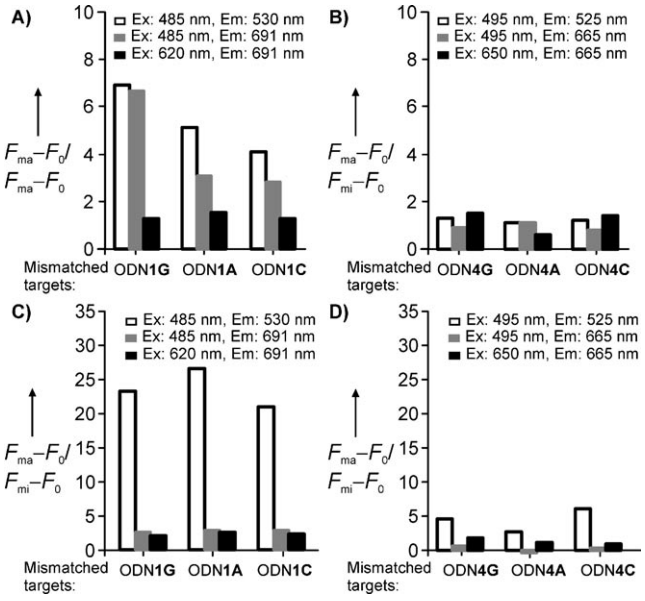

Figure 3. Specificity of fluorescence signaling by probe **1DA** (A, C) and by MB**1** (B, D) presented as the ratio $(F_{ma}-F_0)/(F_{mi}-F_0)$ of the background-corrected fluorescence intensities of matched (F_{ma}) and single mismatched (F_{mi}) probe–target duplexes (F_0 = fluorescence of single strand). A), B) 25 °C and C), D) 65 °C. Conditions: A), C) see Figure 2 and B), D) 1 μM probe and target in 10 mM Tris-HCl, 30 mM KCl, 2 mM $MgCl_2$, pH 9.2; Tris = $(HOCH_2)_3CNH_2$.

We next explored the potential of the stemless PNA beacons in RNA detection. The dual-labeled probe **4DA** was directed against a segment of TAR-RNA, which is responsible for regulation of human immunodeficiency virus (HIV) replication.[9] Hybridization of **4DA** with matched RNA resulted in strong 25- and 32-fold enhancements of TO and NIR667 emission, respectively (Figure 4A). To evaluate whether other dyes of the thiazole orange family can be used as environmentally sensitive donors, oxazole yellow (YO) was incorporated in **5DA**.[10] Again, fluorescence of

 © 2008 Wiley-VCH Verlag GmbH & Co. KGaA, Weinheim

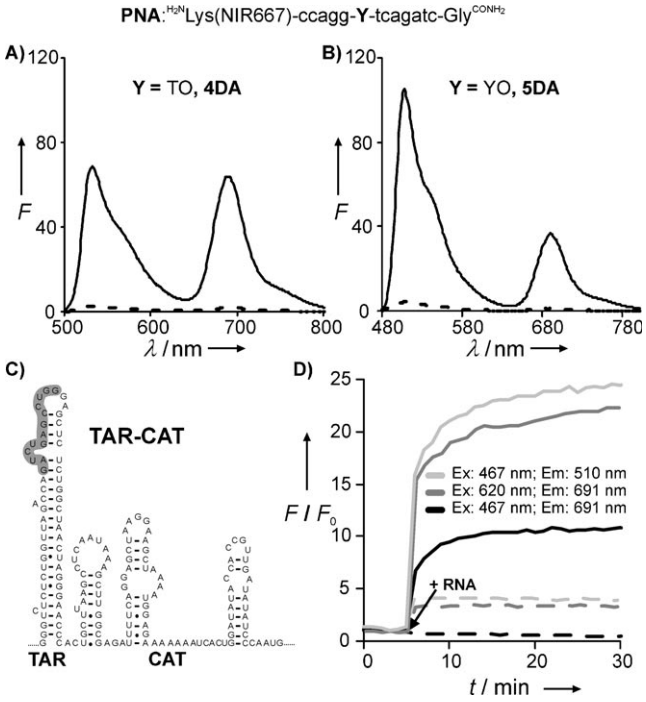

Figure 4. Emission spectra of A) TO-containing probe **4DA** and B) YO-containing probe **5DA** before (dashed line) and after (solid line) addition of matched synthetic RNA. Conditions: 1 μM probes and 2 μM RNA target in buffer (20 mM Tris-HCl, 2.5 mM $MgCl_2$, 12.5 mM NaCl, 1 mM dithiothreitol, pH 6.8, 25 °C, λ_{Ex} = 485 nm for TO and λ_{Ex} = 467 nm for YO). C) Proposed secondary structure of a part of the in vitro transcribed T7-TAR-CAT plasmid and targeted region (shaded in gray). D) Time course of fluorescence emission of **5DA** before and 6 min after addition of TAR-CAT RNA (solid lines) or negative control, total RNA from green alga *Chlamydomonas reinhardtii* (dashed lines). Conditions: 30 nM **5DA** in buffer solution (see conditions for (A) and (B)) and after addition of 300 nM RNA.

5DA was efficiently quenched in the single-stranded form (Figure 4B). Both YO and NIR667 emission responded to RNA hybridization by showing 30- and 38-fold increases of fluorescence. In a model study, we used probe **5DA** to detect a 650 nt long, in vitro transcribed RNA target (Figure 4C) which spanned the TAR loop of the HIV genome within a TAR-CAT fusion.[11] We assumed that **5DA** would be able to bind the TAR-CAT RNA by opening the TAR loop at the highlighted region. Indeed, hybridization of **5DA** with TAR-CAT was accompanied by 24- and 11-fold increases of YO and NIR667 emission, respectively, when excited at the YO absorption wavelength (467 nm, Figure 4D). Fluorescence signalling was a fast process even at 25 °C, thus illustrating the potential of PNA to invade base-paired targets.[12] The nontarget control RNA led to a fivefold increase of YO emission but had no effect on the FRET signal, as NIR667 emission remained virtually unchanged. Excitation at the NIR667 absorption wavelength (620 nm) resulted in a 22-fold fluorescence increase upon hybridization with TAR-CAT RNA but also in a fourfold intensification with the control RNA. Thus, when corrected for nonspecific background, FRET signaling showed a higher fluorescence response, presumably because FRET requires the formation of a complete duplex structure in which neither donor nor acceptor fluorescence can be quenched by dye–dye or dye-nucleobase contacts.

We have shown that stemless PNA beacons are amongst the most sensitive hybridization probes reported to date, as evidenced by up to 10^2-fold fluorescence enhancements upon hybridization. A unique feature of the presented stemless PNA beacons, which is not offered by DNA molecular beacons, is the combination of highly sensitive DNA detection with the possibility to distinguish matched from mismatched target at low temperatures, where both matched and mismatched probe–target duplexes coexist. The dual-labeled hybridization probes provide three different readout modes to detect target DNA and RNA: A) use of TO or YO excitation and emission (ex: 467 or 485 nm, em: 510 or 530 nm), B) use of NIR667 excitation and emission (ex: 620 nm, em: 691 nm) and C) use of FRET at YO or TO excitation and NIR667 emission (ex: 467 or 485 nm, em: 691 nm). Modes B and C showed very high fluorescence enhancements upon hybridization. Mode A provided best mismatch discrimination, even at nonstringent hybridization conditions. It is a notable feature that the distance between the two interacting dyes in stemless PNA beacons is shorter than in molecular beacons. This facilitates FRET-based signaling (mode C), which is in fact described for the first time to afford up to 10^2-fold signal increases with single-nucleotide specificity.[13] Mode C also provided the highest responsiveness over nonspecific background in hybridization experiments with folded RNA targets in complex buffer systems. Based on the very high target specificity and the very high apparent Stokes shift (greater than 200 nm), FRET-based signaling may be preferred when nucleic acid targets are to be detected in biogenic matrices. Direct readout of TO emission (mode A) should be preferred in single-base-mutation analyses, as this mode provides very high (up to 25-fold) mismatch discrimination. The comparison with our previous single-labeled FIT–PNA reveals an extended applicability to various sequence contexts. The omission of a stem segment may facilitate the avoiding of cross-hybridization with non-target sequences.[14] In brief, the observed shift of the emission wavelength from the intercalator dye to the near infrared dye, the high sensitivity, and the high specificity at nonstringent conditions may be useful for reducing background in single-base-mutation analyses and in live-cell RNA imaging.

Received: July 21, 2008
Published online: October 23, 2008

Keywords: FRET · hybridization · molecular beacons · RNA · single-nucleotide polymorphism

[1] a) M. M. Shi, *Clin. Chem.* **2001**, *47*, 164–172; b) T. G. Drummond, M. G. Hill, J. K. Barton, *Nat. Biotechnol.* **2003**, *21*, 1192–1199; c) N. L. Rosi, C. A. Mirkin, *Chem. Rev.* **2005**, *105*, 1547–1562; d) I. M. Mackay, K. E. Arden, A. Nitsche, *Nucleic Acids Res.* **2002**, *30*, 1292–1305; e) D. P. Bratu, B. J. Cha, M. M. Mhlanga, F. R. Kramer, S. Tyagi, *Proc. Natl. Acad. Sci. USA* **2003**, *100*, 13308–13313; f) K. Nakatani, *ChemBioChem* **2004**, *5*,

 © 2008 Wiley-VCH Verlag GmbH & Co. KGaA, Weinheim

1623 – 1633; g) A. P. Silverman, E. T. Kool, *Trends Biotechnol.* **2005**, *23*, 225 – 230.
[2] a) C. J. Yang, H. Lin, W. Tan, *J. Am. Biotechnol.* **2001**, *19*, 365 – 370; b) D. J. Maxwell, J. R. Taylor, S. Nie, *J. Am. Chem. Soc.* **2002**, *124*, 9606 – 9612.
[3] S. Tyagi, F. R. Kramer, *Nat. Biotechnol.* **1996**, *14*, 303 – 308.
[4] a) G. Bonnet, S. Tyagi, A. Libchaber, F. R. Kramer, *Proc. Natl. Acad. Sci. USA* **1999**, *96*, 6171 – 6176; b) T. N. Grossmann, L. Röglin, O. Seitz, *Angew. Chem.* **2007**, *119*, 5315 – 5318; *Angew. Chem. Int. Ed.* **2007**, *46*, 5223 – 5225.
[5] Previous stemless beacons: a) E. Ortiz, G. Estrada, P. M. Lizardi, *Mol. Cell. Probes* **1998**, *12*, 219 – 226; b) O. Seitz, F. Bergmann, D. Heindl, *Angew. Chem.* **1999**, *111*, 3674 – 3677; *Angew. Chem. Int. Ed.* **1999**, *38*, 3466 – 3469; c) O. Seitz, *Angew. Chem.* **2000**, *112*, 3389 – 3392; *Angew. Chem. Int. Ed.* **2000**, *39*, 3249 – 3252; d) H. Kuhn, V. V. Demidov, J. M. Coull, M. J. Fiandaca, B. D. Gildea, M. D. Frank-Kamenetskii, *J. Am. Chem. Soc.* **2002**, *124*, 1097 – 1103; e) E. Privat, T. Melvin, U. Asseline, P. Vigny, *Photochem. Photobiol.* **2001**, *74*, 532 – 541; f) O. Köhler, D. V. Jarikote, O. Seitz, *ChemBioChem* **2005**, *6*, 69 – 77; g) N. Svanvik, G. Westman, D. Y. Wang, M. Kubista, *Anal. Biochem.* **2000**, *281*, 26 – 35; h) E. Ergen, M. Weber, J. Jacob, A. Herrmann, K. Müllen, *Chem. Eur. J.* **2006**, *12*, 3707 – 3713.
[6] a) D. V. Jarikote, N. Krebs, S. Tannert, B. Röder, O. Seitz, *Chem. Eur. J.* **2007**, *13*, 300 – 310; b) V. Karunakaran, J. L. Pérez Lustres, L. Zhao, N. P. Ernsting, O. Seitz, *J. Am. Chem. Soc.* **2006**, *128*, 2954 – 2962.
[7] a) O. Köhler, O. Seitz, *Chem. Commun.* **2003**, 2938 – 2939; b) O. Köhler, D. V. Jarikote, O. Seitz, *Chem. Commun.* **2004**, 2674 – 2675; c) E. Socher, D. V. Jarikote, A. Knoll, L. Röglin, J. Burmeister, O. Seitz, *Anal. Biochem.* **2008**, *375*, 318 – 330.
[8] a) M. K. Johansson, H. Fidder, D. Dick, R. M. Cook, *J. Am. Chem. Soc.* **2002**, *124*, 6950 – 6956; b) M. K. Johansson, R. M. Cook, *Chem. Eur. J.* **2003**, *9*, 3466 – 3471.
[9] B. Berkhout, *Adv. Pharmacol.* **2000**, *48*, 29 – 73.
[10] L. Bethge, D. V. Jarikote, O. Seitz, *Bioorg. Med. Chem.* **2008**, *16*, 114 – 125.
[11] D. Dorin, M. C. Bonnet, S. Bannwarth, A. Gatignol, E. F. Meurs, C. Vaquero, *J. Biol. Chem.* **2003**, *278*, 4440 – 4448.
[12] a) J. C. Hanvey, N. J. Peffer, J. E. Bisi, S. A. Thomson, R. Cadilla, J. A. Josey, D. J. Ricca, C. F. Hassman, M. A. Bonham, K. G. Au, S. G. Carter, D. A. Bruckenstein, A. L. Boyd, S. A. Noble, L. E. Babiss, *Science* **1992**, *258*, 1481 – 1485; b) P. Wittung, P. Nielsen, B. Nordén, *J. Am. Chem. Soc.* **1996**, *118*, 7049 – 7054.
[13] F. Menacher, M. Ruber, S. Berndl, H. A. Wagenknecht, *J. Org. Chem.* **2008**, *73*, 4263 – 4266.
[14] a) C. Crey-Desbiolles, D. Ahn, C. Leumann, *Nucleic Acids Res.* **2005**, *33*, e77; b) Y. Kim, C. J. Yang, W. Tan, *Nucleic Acids Res.* **2007**, *35*, 7279 – 7287.

 © 2008 Wiley-VCH Verlag GmbH & Co. KGaA, Weinheim